Properties of Magnetically Balanced Arcs

LELAND M. NICOLAI* AND ARNOLD M. KUETHE
Department of Aerospace Engineering, The University of Michigan, Ann Arbor, Michigan
(Received 12 November 1968)

Experimental results on steady magnetically balanced arcs in supersonic external flows are presented and analyzed, along with investigations elsewhere in subsonic flows, to determine the important similarity parameters. The studies indicate that the steady arc has a central core, impervious to the external flow, within which differential Lorentz forces generate a circulation analogous to that generated by gravity forces in nonuniformly heated gas in a horizontal tube. The conservation equations indicate that a "Lorentz convection parameter," analogous to the Grashof number in free convection phenomena, is an important similarity parameter over a significant range of arc variables. A "characteristic velocity" for the core circulation is indicated. The similarity parameters that provide the interpolation between the properties of subsonic and supersonic balanced arcs indicate the approximations permissible for a first-order solution to the internal circulation. It is inferred from the results that to a first approximation the thickness of the enthalpy boundary layer varies linearly with the reciprocal of the Reynolds number of the external flow.

I. INTRODUCTION

Our knowledge of even the gross aspects of mass, momentum, and energy transfer between an arc and an external stream today depends almost completely on empirical data. However, solutions to such practical problems as determination of the mass loss from a gaseous fission reactor, and the maximization of the acceleration in $\mathbf{J}\times\mathbf{B}$ or $\mathbf{E}\times\mathbf{B}$ accelerators will require detailed knowledge of fluid and plasma interactions such as occur at the boundary of a balanced arc. This paper, based, in large part on Refs. 1 and 2, draws upon and extends that reported in Ref. 3; it identifies, through inference from the approximate conservation equations and experimental data, some features of these mechanisms and the governing parameters.

The first instance of a steady arc balanced magnetically in a cross flow of appreciable velocity was reported by Bond in 1962.[4] Subsequent investigations,[5,6] in which fairly intense external magnetic fields were utilized to balance dc arcs in supersonic external flows, led to the determination of the gross properties of these arcs. One of these properties, a slant angle a few degrees greater than the Mach angle of the external flow, was found to occur whenever the arc was steady.[7]

The experimental work presented here utilized the equipment described in Refs. 4–6 and extends the work toward the delineation of a model of the arc as a basis for calculating the fluid mechanical structure of the arc. The equipment provided the field configuration indicated in Fig. 1 in which the arc was initiated by an exploding wire between rail electrodes parallel to the external flow. The balance between the aerodynamic and the Lorentz forces was achieved by means of an external magnetic field oriented normal to the electric field and to the external flow direction.

The works of Roman and Myers,[8,9] show that a steady magnetically balanced arc can be achieved when the arc is generated across a free jet at subsonic air speeds. This "subsonic balanced arc" was generated between coaxial pin electrodes and was normal to the cross flow; it was remarkably steady over a range of arc currents and jet speeds, so that traverses of velocity and enthalpy in the wake could be made.

These measurements at subsonic and at supersonic speeds provide a basis for examining the extent to which the fluid mechanical structure of the

---

* Present address: United States Air Force Academy, Colorado Springs, Colorado.

[1] L. M. Nicolai, Ph.D. dissertation, The University of Michigan (1968).

[2] A. M. Kuethe, R. L. Harvey, and L. M. Nicolai, AIAA Bull. 3, 750 (1966).

[3] R. L. Harvey, Ph.D. dissertation, The University of Michigan (1968).

[4] C. E. Bond, AIAA J. 3, 142 (1963).

[5] C. E. Bond, Ph.D. dissertation, The University of Michigan (1964).

[6] C. E. Bond, Phys. Fluids 9, 705 (1966).

[7] C. E. Bond and R. W. Potillo [AIAA J. 6, 1565 (1968)] recently reported on experiments on arcs convected magnetically along heated rail electrodes. They find, as in the balanced arc tests, that the arc slants at near the Mach angle when the convection speed is supersonic; however, when the speed is subsonic the slant persists, the angle decreasing with speed.

[8] W. C. Roman, Ph.D. dissertation, The Ohio State University (1966).

[9] W. C. Roman and T. W. Myers, AIAA J. 5, 2011 (1967).

balanced arc can be described by the equations of continuum mechanics of a conducting fluid. The experimental data are used to calculate the nondimensional parameters indicated by the momentum and energy equations; the validity of the approximations made are inferred from the behavior of the parameters.

Some limited attempts have been made,[10-13] to attack the problems of the balanced arc by solving the conservation equations for the entire flow field with boundary conditions at infinity. The complete solution would comprise determination of the field properties, internal and external, for a plasma column whose boundaries are determined by the equilibrium conditions between the internal and external pressure fields. The problem is incomparably more difficult than that of the flow around a body of fixed dimensions. For the arc, even if the cross-section shapes are known, the boundary conditions necessary for calculating the flow in the boundary layer and, particularly, near the flow separation point are not. Accordingly, one is forced to seek a model of the arc which will provide a framework for calculating the arc properties under circumstances which can be checked by experiment.

The experimental results were used to evaluate the nondimensional parameters that occur in the conservation equations. The functional relationships which emerge indicate that there is a range of field properties over which the internal circulation can be determined to first order by means of solutions of the conservation equations for incompressible flow of a conducting fluid, neglecting effects of radiation, nonequilibrium, and of the current induced by the motion of the conducting fluid through the induced and applied magnetic force field.

The experimental results given here are analyzed, along with those of other investigators,[8,9,14] to indicate, on the basis of simplified conservation equations, the main features of the fluid mechanical structure of the steady balanced arc and the governing similarity parameters. The results are consistent with the following description: For low cross-flow velocities the internal processes are substantially those of the free-burning arc, but as the cross flow

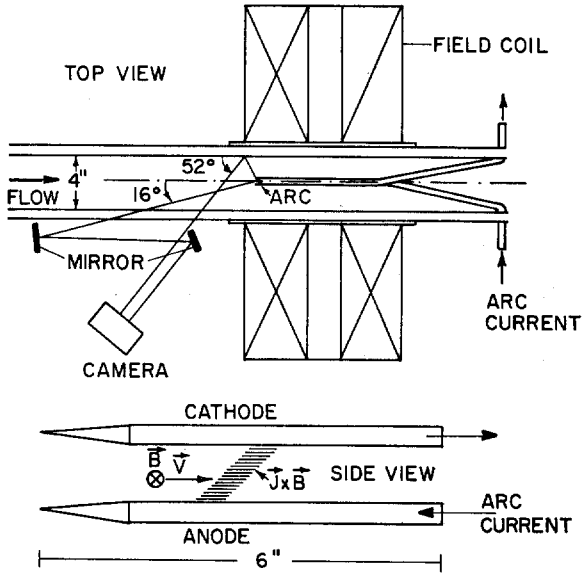

FIG. 1. Top view of experimental setup with enlarged view of arc with field directions.

increases the magnetic field required to maintain force balance causes an internal circulation to develop within a core of relatively uniform properties; under these conditions the transfer of energy, momentum, and mass to the external flow takes place mainly through relatively thin boundary layers over the upstream boundary of the core. By inference, the boundary-layer thickness at the upstream boundary is compared with that of a solid heated cylinder.

II. MEASURED ARC PROPERTIES

A. Equipment and Scope

The experimental apparatus shown schematically in Fig. 1, consisted of cone–cylinder rail electrodes mounted in the 4 × 4 in. variable Mach number supersonic wind tunnel at The University of Michigan. Water cooled field coils provided the transverse magnetic field required to balance the aerodynamic force on the arc. These coils and other features of the adaptation of the tunnel to a balanced arc investigation are described by Bond.[4,5] For the results reported here the optical arrangement shown in Fig. 1 was used permitting two simultaneous exposures to be taken, thus facilitating measurements of arc dimensions.

The measurements on which the arc dimensions and slant angles given here are based were taken at Mach numbers 2.5, 3.0, and 3.5 at stagnation pressures, respectively, 320, 530, and 730 Torr and at atmospheric temperatures. For purposes of standardization relative to the dimensions of the luminous

[10] P. G. Thiene, Phys. Fluids **6**, 1319 (1963).
[11] V. W. Adams, A. E. Guile, W. T. Lord, and K. A. Naylor, in *Proceedings of the Eighth International Conference on Phenomena in Ionized Gases* (Springer-Verlag, Berlin, 1967), p. 246.
[12] W. T. Lord, J. Fluid Mech. **35**, 689 (1969).
[13] E. Fischer and J. Uhlenbusch, in *Proceedings of the Seventh International Conference on Phenomena in Ionized Gases* (Gradevinska Knija, Beograd, Yugoslavia, 1966), p. 725.
[14] Y. Y. Winograd and J. F. Klein, AIAA J. (to be published).

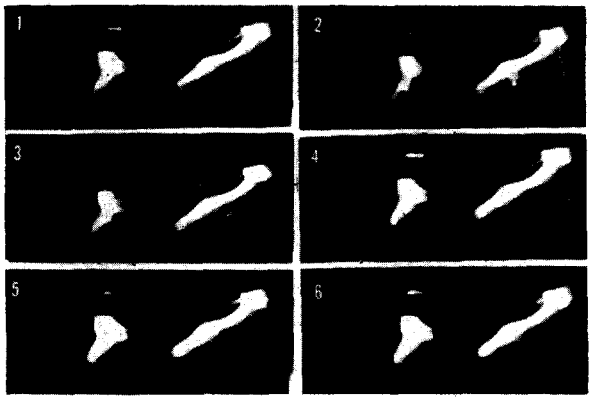

FIG. 2. Sequence of two-view photographs showing motion of vaporizing magnesium particle in wake of arc. Mach number 3.5, 4500 exposures/sec.

regions the photographs were taken with a Nikon camera at $f/11$ at 10^{-3} sec with Kodak Panatomic-X film.

The Mach numbers and stagnation pressures of the tests were within the range where steady arcs could be achieved. There were at each Mach number ranges of stagnation pressure, gap, and current, outside of which the arc became quite unsteady as evidenced by the high-speed motion pictures and by the measured current and voltage drop. Bond's results[4,6] indicated that the lower pressure and higher current limitations are caused by thermal choking of the tunnel. At Mach numbers of 2.0 and 4.0 it was possible only very occasionally to strike a steady arc; the stagnation pressures at the three Mach numbers above were chosen because they are well within the range for steady arcs for the gaps and currents used. It should be remarked that even within the favorable ranges the arc was for no apparent reason occasionally unsteady, but outside of the favorable ranges it was invariably unsteady.

B. The Arc as an Impervious Cylinder

The tracer studies described here and in Refs. 2 and 3, along with the measurements of Refs. 8 and 10, show the existence of an impervious core within a steady balanced arc.

For instance, Fig. 2 shows a sequence of simultaneous near-side and near-frontal images in which the motion of a vaporizing particle of magnesium is shown; the first appearance of the particle is immediately behind the arc in frame 2.[15] The succeeding frames show the subsequent motion of the particle along a path inclined only slightly to the arc. A low relative speed in the wake is thus indicated by the fact that if the particle moved with the external flow speed (around 1800 ft/sec), the exposure frequency of 4500/sec would show a travel of about 4 in. between exposures. Other high-speed motion pictures[2,3] indicate the motion of vaporizing particles along the interior of the column at speeds around 30 ft/sec. These measurements, because of the inertia of the particles, give a lower bound for the axial velocities; however, the mere existence of the flow along the arc under conditions for which the arc plasma and the external flow are effectively continua is proof that the arc is impervious to the external flow.

Roman[8] and Myers[9] in their investigations of a balanced arc normal to a low-speed flow observed flow separation at about 90° from the forward stagnation point and a practically stagnant region directly behind the arc. In addition, they found spectroscopically that the radiation from the arc was practically pure argon, which was introduced at the cathode to inhibit oxidation.

The conclusion from all of the above observations is that the steady balanced arc comprises an impervious core from which mass (supplied by an axial flow), momentum, and energy are transferred through a boundary layer to the external flow. Later we are concerned with conditions under which a *thin* boundary layer may be hypothesized.

C. Arc Slant and Dimensions

When the cone–cylinder electrodes were used, the steady arc in the supersonic flow always slanted with the anode root upstream. In the earlier work[3,4] the slant was taken as the inclination of the line connecting the anode and cathode roots; it was found that the slant angle was within a few degrees of the Mach angle. For the more recent observations,[1] however, the slant, as well as the representative arc dimensions and the magnetic field strengths, were taken as the values at the point one-third of the distance from anode to cathode; Fig. 2 shows that the leading edges of the reflected images have nearly constant slant and dimensions in the region of this reference location. Further support for this choice of reference location lies in the consistency of the

[15] The photographs (see the schematic view of Fig. 3) show that the arc extends from the anode rail (bottom) toward, then curls around, the cathode rail to the cathode root at about 120° from the point nearest the anode. Factors tending to cause this "curling" behavior are: a cross-stream component of the Lorentz force,[5] the Lorentz force acting on the cathode jet tending to move it to a point where the jet is parallel to the magnetic lines of force, buoyancy and shear forces on the arc column establishing an axial flow which will tend to remain coherent on one side or the other of the cathode rail.

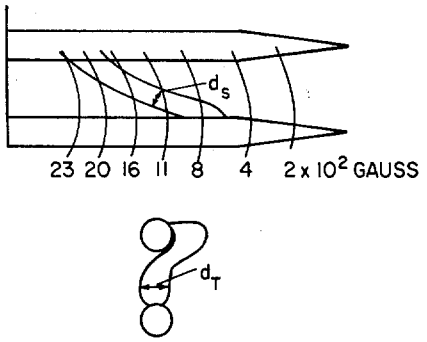

FIG. 3. Tracing of arc (Mach 3.5) showing side (d_S) and transverse (d_T) dimensions and surfaces of constant magnetic induction in the plane of the arc.

results presented later. Schematic head-on and side views and isomagnetic field contours are shown in Fig. 3. Figure 4 shows a log–log plot of the slant angles for three Mach numbers and indicates that slant angle is proportional to $I^{0.25}$. Over the range of the observations the slant angle at a given Mach number is nearly proportional to $U_{\infty n}$, the velocity component normal to the leading edge; thus the results indicate that $U_{\infty n}$ is proportional to $I^{0.25}$ at a given Mach number at constant stagnation pressure and temperature.

The log–log plot of Fig. 5 shows that d_S and d_T, the streamwise and transverse dimensions (see Fig. 3) are proportional to $I^{0.5}$. The measurements were made by means of the mirror arrangement shown in Fig. 1, corrected for the viewing angle. The boundaries (see Fig. 2) are well defined for the upstream image but the rear boundaries are less distinct. Since the image on the film represents an integrated luminosity along a line of sight, the indicated temperature at the edge of a luminous region will depend on the luminosity or temperature gradients in the vicinity; if we assume steep gradients; temperature estimates over the upstream arc boundary vary from 6000°K for subsonic balanced arc tests[8] to 7200°K for the supersonic arc tests presented here.[1]

The values of d_S and d_T shown in Fig. 5 increase with $I^{0.5}$ for each Mach number (for constant stagnation temperature and pressure), indicating that if the cross sections and current density distributions are similar the average current densities are constant for a given Mach number (see Sec. IIE).

The cause of the arc slant is not known; Bond and Potillo[7] find that a traveling arc in a uniform field slants and Winograd and Klein[14] find that the slant also occurs on rail electrodes in a subsonic external flow. The use of blunt and sharp electrodes in a supersonic flow[1] indicates that both the direction

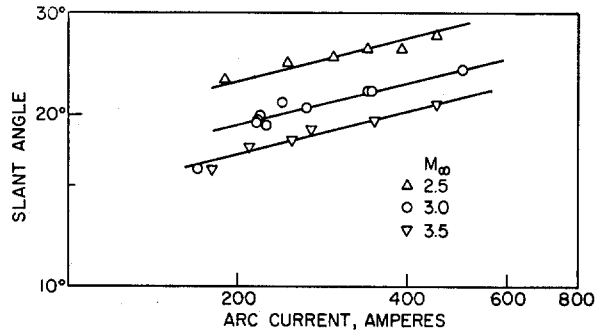

FIG. 4. Slant angle of the arc at the reference station.

and magnitude of the slant are affected by the shock wave configurations around the electrodes. These various tests support Bond's conclusion[6] that Hall currents have negligible effect on the slant.

D. Electric Field Measurements

The electric fields were measured in the standard manner; records were made with two different gaps, 0.6 and 1.0 in., and the measured total voltages were subtracted to obtain the voltage drops along the column. Consistent results were obtained only after discarding runs for which the voltage trace showed the slightest unsteadiness. The resulting data are shown in Fig. 6, in which results reported by Bond are shown for comparison; the pressures given are the ambient pressures at the respective Mach numbers. An interesting feature of Fig. 6 is that for a given M_∞ the E is fairly constant for increasing current, in spite of the fact, pointed out in section 2c, that $U_{\infty n}$ varies with arc current.

E. "Effective" Arc Properties

A mean current density over the luminous portion of the arc is given by

$$J_1 = I/\tfrac{1}{4}\pi\, d_T\, d_S. \qquad (1)$$

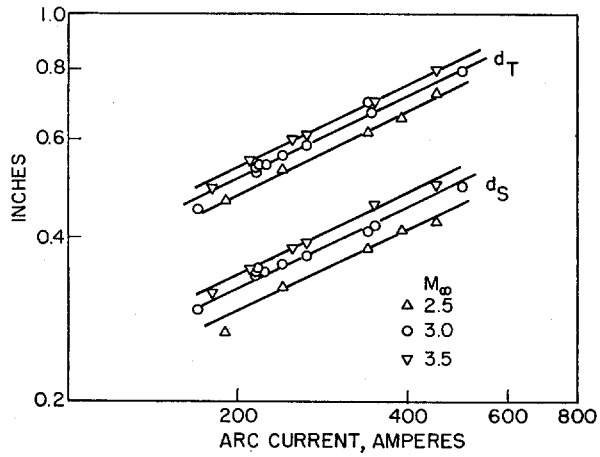

FIG. 5. Dimensions of the arc at the reference station.

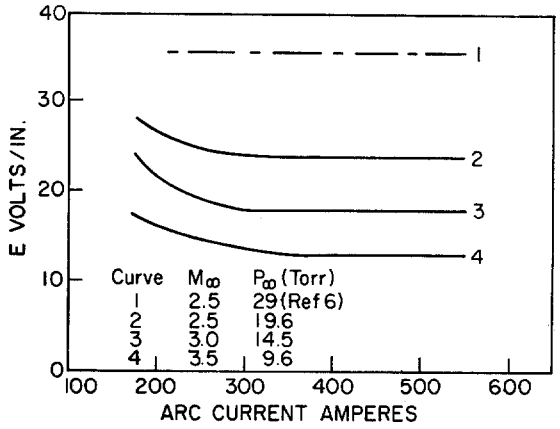

FIG. 6. Voltage gradient along the arc.

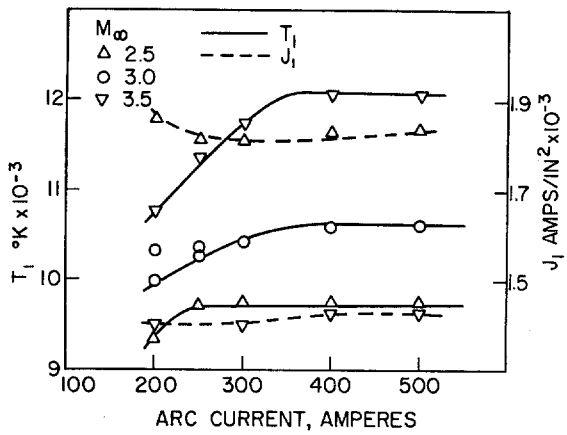

FIG. 7. Reference temperature and current density within the arc.

An effective arc temperature T_1, defined as the temperature corresponding to an effective electrical conductivity σ_1, is given by

$$\sigma_1(T_1, P_\infty) = J_1/E. \tag{2}$$

These properties are plotted versus current in Fig. 7. Values of T_1 were taken from published transport data.[16-18]

III. MODEL OF THE BALANCED ARC

A. Qualitative Description

The properties of the slanted balanced arc at the reference point shown in Fig. 3 are assumed to approximate those of an infinite cylinder of uniform elliptical cross section in a uniform magnetic field oriented normal to a cross flow of velocity $U_{\infty n}$, the component of the undisturbed flow normal to the

[16] B. Ragent and C. E. Nobel, ARL Report 62-328 (1962).
[17] J. Hilsenrath and M. Klein, AEDC Technical Report 65-58 (1965).
[18] K. S. Drellishak, C. F. Knopp, and A. B. Cambel, Phys. Fluids 6, 1280 (1963).

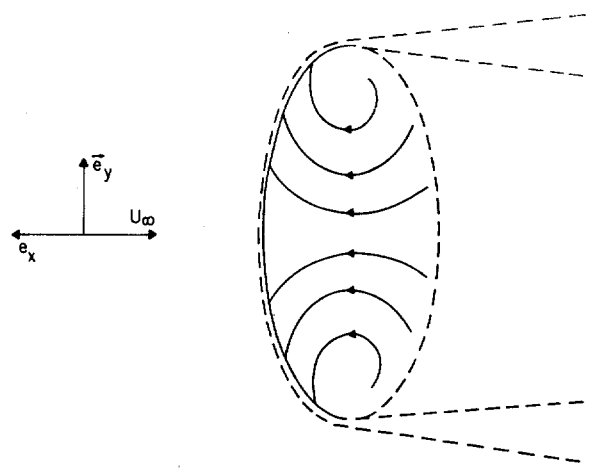

FIG. 8. Schematic projections of internal streamlines on transverse plane of arc model. Flow separation shown as measured in Ref. 9.

axis. This model, described in Ref. 2, is shown schematically in cross section in Fig. 8; it comprises an impervious elliptical core and a boundary layer over the upstream boundary through which mass, energy, and momentum are transferred to the external flow. Flow separation at the maximum section is in conformity with the wake traverses of Roman and Myers and is consistent with the small wake velocities indicated in Fig. 2.

The internal circulation shown in Fig. 8 represents the projections on the cross section of streamlines of the flow generated by the differential Lorentz forces acting on the plasma elements. The force field associated with nonuniform current density in a uniform magnetic field in the y direction sets up a "Lorentz circulation," conceptually analogous to the circulation set up by the gravity field acting on a centrally heated horizontal cylinder of gas. Specifically, an element will be accelerated toward the upstream boundary if its current density is greater than that required to just balance the pressure gradient within the arc, and *vice versa* for those plasma elements with current density insufficient for the force balance. Also, the pressure gradient along the boundary will propagate into the interior and deflect fluid elements laterally. The combined effects of these influences will be to set up a circulation such as is shown in Fig. 8.

The Joule heating, for which there is no counterpart in the natural convection analogy, tends to cause the temperature and, therefore, the current density and Lorentz force on an element to increase as the element moves upstream within the core where heat conduction is small. Thus, the effect of the Joule heating will be to intensify the internal

circulation, and to generate high-temperature gradients at the upstream boundary.

The calculated internal circulation and its effect on the temperature distribution is shown for a simplified model in Fig. 9.[3] The results were obtained as part of an extension of the computer study of Ref. 13 of an arc in a circular tube with a uniform magnetic field normal to its axis; the work was undertaken as a first approximation to the structure of the core of the balanced arc column. The contours show the effect of the internal circulation in moving the maximum temperature point toward the upstream boundary of a balanced arc. Further calculations, reported in Refs. 1 and 3, will be published separately.

The balanced arc will assume a shape such that the fluid pressure in the external flow equals the fluid plus magnetic pressure at the arc boundary. The internal properties become steady when an equilibrium current density or temperature distribution is reached such that the internal circulation and conduction are sufficient for transfer of the heat generated to (mainly) the upstream boundary where the transfer of the heat generated takes place through a relatively high temperature gradient.

The apparent dimensions of the arc as given by the boundaries of the luminous region are shown in Fig. 5. As mentioned in the previous section temperature estimates of the upstream boundary vary from 6000° to 7200°K. These temperatures are near the threshold values above which the electrical conductivity becomes appreciable. Thus, the photographic image is assumed to define an isotherm within which the major part of both the Joule heating and Lorentz body force occur. Exterior to this region the Lorentz force vanishes and the gas is acted on only by pressure and viscous forces. The properties of the flow in this boundary region will be determined by the energy, mass, and momentum transferred from the core.

B. Quantitative Description of Core

The most important hypotheses incorporated in the model described above are: (1) the arc core and boundary layer may be treated separately, (2) the core of the slanted arc column may be treated as an inclined cylinder of uniform elliptical cross section in a uniform magnetic field, (3) as a result of the Lorentz circulation the properties of the plasma within the core are sufficiently uniform so that characteristic values may be taken as the "effective" values (Sec. IIE) over the cross section at a reference location, and (4) the characteristic external velocity is that normal to the arc axis.

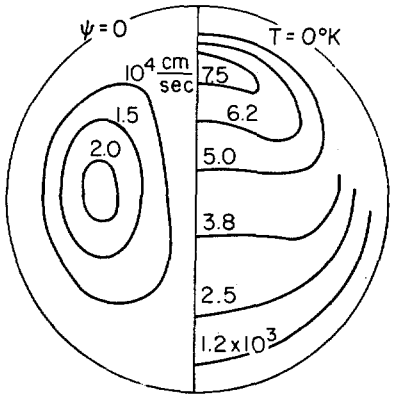

FIG. 9. Calculated streamlines and isotherms by Harvey[3] for arc in circular tube in uniform magnetic field ($\mathbf{J} \times \mathbf{B}$ positive upward). $K_{JH} = 5 \times 10^3$, $L_c = 1.1 \times 10^2$.

In the following paragraphs the available experimental data, analyzed on the basis of simplified conservation equations, is the basis for determining a range of parameters over which the model effectively approximates the structure of the arc column. The simplifications are carried out around the equations for a weakly ionized gas in which radiation and nonequilibrium effects are neglected. These two-dimensional equations, relative to coordinates in the plane normal to the column axis, are

$$\nabla \cdot \rho \mathbf{V} = \epsilon, \tag{3}$$

$$\rho(\mathbf{V} \cdot \nabla)\mathbf{V} = -\nabla P + \mathbf{J} \times \mathbf{B} + \frac{\partial \tau_{ij}}{\partial x_i}, \tag{4}$$

$$\rho(\mathbf{V} \cdot \nabla H) = \mathbf{V} \cdot \nabla P + \nabla^2 \Phi + J^2/\sigma + \psi, \tag{5}$$

where ϵ is the source strength (mass drawn from the axial flow to balance mass transfer at the boundary), $\mathbf{V}$ is the velocity vector $(u, v, 0)$, τ_{ij} is the viscous stress tensor, $H = \int c_p \, dT$ is the static enthalpy $\Phi = \int k \, dT$ is the heat flux potential, ψ is the viscous dissipation rate, $P = Z\rho RT$ is the pressure, Z is the compressibility factor, ρ is the density, R is the gas constant, T is the absolute temperature, c_p is the specific heat at constant pressure, k is the heat conduction coefficient, $\mathbf{J}$ is the electric current density, σ is the electric conductivity, and $\mathbf{B}$ is the magnetic induction.

Numerical results[1] show that the $\mathbf{V} \times \mathbf{B}$ term in Ohm's law is for all practical purposes, negligible compared with $\mathbf{E}$, the electric field, so that

$$\mathbf{J} = \sigma (\mathbf{E} + \mathbf{V} \times \mathbf{B}) \simeq \sigma \mathbf{E}. \tag{6}$$

Equations (3)–(5) are nondimensionalized by the use of characteristic values V_1, H_1, ρ_1, Φ_1, σ_1, J_1, and length d_1, to get for $\mu = \mu_1 = \text{const}$,

$$\nabla \cdot (\rho' \mathbf{u}) = \epsilon \, d_1 / P_1 V_1, \tag{7}$$

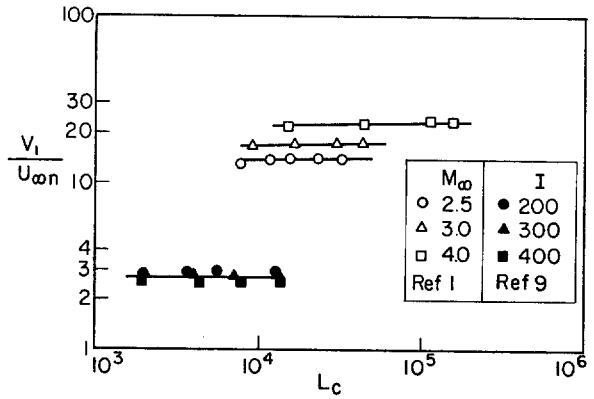

FIG. 10. Characteristic velocity parameter for internal circulation in subsonic and supersonic cross flows.

$$\rho'(\mathbf{u}\cdot\nabla)\mathbf{u} = -\nabla p + \frac{L_c}{\mathrm{Re}^2} j\mathbf{e}_x + \frac{1}{\mathrm{Re}}\nabla^2\mathbf{u} + \frac{1}{3\,\mathrm{Re}}\nabla(\nabla\cdot\mathbf{u}), \tag{8}$$

$$\rho'(\mathbf{u}\cdot\nabla h) = K\mathbf{u}\cdot\nabla p + \frac{1}{\mathrm{Pr}\,\mathrm{Re}}\nabla^2\phi + K_{JH}j + \frac{K}{\mathrm{Re}}\psi_1, \tag{9}$$

where

$$\rho' = \frac{\rho}{\rho_1}, \qquad \mathbf{u} = \frac{\mathbf{V}}{V_1},$$
$$p = \frac{P}{\rho_1 V_1^2}, \qquad h = \frac{H}{H_1}, \tag{10}$$
$$\phi = \frac{\Phi}{\Phi_1}, \qquad j = \frac{J}{J_1},$$

and the operator ∇ is nondimensionalized with d_1. The similarity parameters are $K = V_1^2/H_1$ is the Eckert number, $\mathrm{Pr} = \mu_1 H_1/\Phi_1$ is the Prandtl number, $\mathrm{Re} = \rho_1 V_1 d_1/\mu_1$ is the Reynolds number, $K_{JH} = \sigma_1 E^2\, d_1/\rho_1 V_1 H_1$ is the Joule heating parameter, and $L_c = \rho_1 J_1 B\, d_1^3/\mu_1^2$ is the Lorentz convection parameter.

A consistent set of electrical and thermodynamic characteristic properties includes T_1, J_1, σ_1 [see Eqs. (1) and (2) and Fig. 7] H_1, and Φ_1. For the latter two the integrals are taken from the external ambient temperature to T_1; c_p and k are given in Refs. 16, 17, and 18. It is assumed that the temperature variation over the core cross section is small enough so that $\mu = \mu_1$ is constant.

The characteristic length is taken as

$$d_1 = (\tfrac{1}{4}\pi d_s d_T)^{1/2}. \tag{11}$$

The characteristic velocity V_1 was chosen on the basis of the analogy between Lorentz and natural convection; it is taken as proportional to the velocity acquired by a fluid element acted on by a Lorentz force $J_1 B$ over a distance d_1, that is,[19]

$$V_1 = (J_1 B\, d_1/\rho_1)^{1/2} = (IB/\rho_1\, d_1)^{1/2}. \tag{12}$$

It was shown in Ref. 3 that $V_1/U_{\infty n}$ has nearly constant values for Mach numbers 2.5 and 3.5 and for the subsonic measurements of Roman and Myers. The measurements of Ref. 1 shown in Fig. 10 show the same feature. Thus, the velocity V_1 is *in fact* a characteristic property for a given Mach number and over a significant range of subsonic velocities.

The similarity parameters in Eq. (18) refer to characteristic properties within the arc core. For instance, for constant c_p, the Eckert number $V_1^2/H_1 = (\gamma - 1)M_1^2$, where M_1 is a characteristic Mach number for the core flow. The Reynolds number becomes, after substituting for V_1 from Eq. (12)

$$\mathrm{Re} = (\rho_1 J_1 B\, d_1^3/\mu_1^2)^{1/2} = (L_c)^{1/2}. \tag{13}$$

The parameter L_c, termed the "Lorentz convection parameter," is, with the help of Eq. (12), interpreted physically as the square of the ratio of the Lorentz force, $J_1 B$, to the viscous force, $\mu_1 V_1/d_1^2$, acting on a representative volume element.[20] We would, therefore, expect that the magnitude of L_c would determine the intensity of the internal circulation.

The "Joule heating parameter" K_{JH} can be expressed as

$$K_{JH} = \frac{EI/\Phi_1}{\mathrm{Pr}\,(L_c)^{1/2}}, \tag{14}$$

where EI/Φ_1 is proportional to the ratio of the rate at which an element is heated by electric dissipation, EJ_1, to Φ_1/d_1^2, the rate at which heat is conducted from the element.

Equations (7)–(9) are assumed to apply to the slanted arc as well as to the arc oriented normal to the external flow at stations well removed from the root regions of columns having large ratios of length to major lateral dimension. Since the axial flow must supply the fluid lost through mass transfer to the external flow, this rate of mass transfer must be small relative to the flow rate along the column if

[19] In natural convection problems the Lorentz force is replaced by the gravity force. See for instance, S. Ostrach, in *High Speed Aerodynamics and Jet Propulsion*, F. K. Moore, Ed. (Princeton University Press, Princeton, New Jersey, 1964), Vol. II, Sec. F.

[20] In natural convection, if a characteristic velocity analogous to Eq. (12) is used, the ratio of gravity force to viscous force on a heated fluid element becomes the square root of the Grashof number.

the two-dimensional flow approximation is to be valid. Specifically, the right-hand side of Eq. (7) must be small.

High core temperatures, leading to low internal Mach numbers,[1] justify the neglect of the last term in Eq. (8) and of the pressure work term in Eq. (9). Also, the internal circulation will tend to decrease gradients in the core, so that the viscous dissipation term in Eq. (9) may be neglected. Then, after introducing Eqs. (13) and (14), Eqs. (8) and (9) becomes

$$\rho'(\mathbf{u}\cdot\nabla)\mathbf{u} = -\nabla p + j\mathbf{e}_x + \frac{1}{(L_c)^{1/2}}\nabla^2\mathbf{u}, \qquad (15)$$

$$\rho'(\mathbf{u}\cdot\nabla h) = \frac{1}{\Pr\,(L_c)^{1/2}}\nabla^2\phi + \frac{EI/\Phi_1}{\Pr\,(L_c)^{1/2}}j. \qquad (16)$$

As the force required to balance the arc approaches zero $B \to 0$ and, therefore, $L_c \to 0$. Then, the circulation within the arc vanishes and the only remaining equation with nonzero terms is Eq. (16), which becomes the "Elenbaas–Heller" equation,[21]

$$(EI/\Phi_1)j = V^2\phi. \qquad (17)$$

This equation governs the temperature distributions for free-burning and for wall stabilized arcs.

For large L_c, Eqs. (15) and (16) are of the boundary-layer type; that is, the coefficients of the highest-order terms are small compared with those of the convective terms. As a consequence there will be, at the core boundary, thin boundary layers in velocity and static enthalpy. It follows that $L_c \gg 1$ is the condition for nearly constant properties within the arc core; the conduction term in Eq. (16) will then vanish and if the heating rate is to remain finite, limiting conditions are

$$(L_c)^{1/2} \to \text{const}\,\frac{EI}{\Phi_1\,\Pr}, \quad \text{or} \quad K_{JH} \to \text{const}. \qquad (18)$$

In the next section these results are compared with experiment for subsonic and supersonic arcs.

IV. COMPARISON WITH EXPERIMENT

The low-speed data of Roman and Myers and the high-speed data presented here are plotted in Fig. 11 as a test of the validity of the limiting conditions of Eq. (18). While there is a systematic variation with Mach number, the supersonic results are described reasonably well by the straight line with a slope of 0.5, as specified by Eq. (18). The subsonic results, on the other hand, show significant deviations: at low L_c the curves approach zero slope where

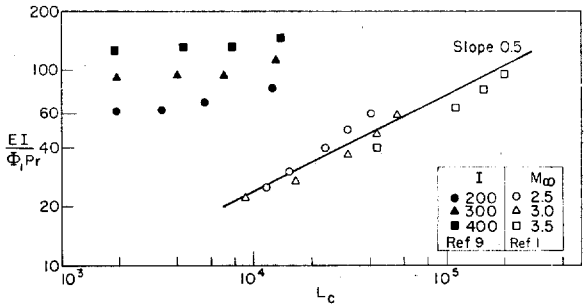

FIG. 11. Test for constancy of Joule heating parameter for subsonic and supersonic cross flows.

the values of $EI/\Phi_1\Pr_1$ are roughly proportional to the arc current; at intermediate L_c where the subsonic and supersonic ranges overlap there is an indication that the subsonic data may be approaching the 0.5 slope; in the overlap region of L_c, the subsonic $EI/\Phi_1\ \Pr_1$ is about four times that for the supersonic results.

The experimental conditions as well as the magnitudes of the velocities and pressures are significantly different for the two sets of experiments. Values of k for argon[16,18] were used for the Roman–Myers subsonic data (see Sec. IIB) while those for air[16,17] were used for the supersonic data; also the supersonic arc slanted while the subsonic was normal to the cross flow.

In spite of these differences it was found that the two sets of data could be brought together by introducing the electric field E_0 for the free-burning arc. While E_0 varies with current for $I < 100$ A, it is found to be constant over the current ranges used in the balanced arc measurements. Figure 12 shows E_0 as a function of the ambient pressure[1] P_∞; the

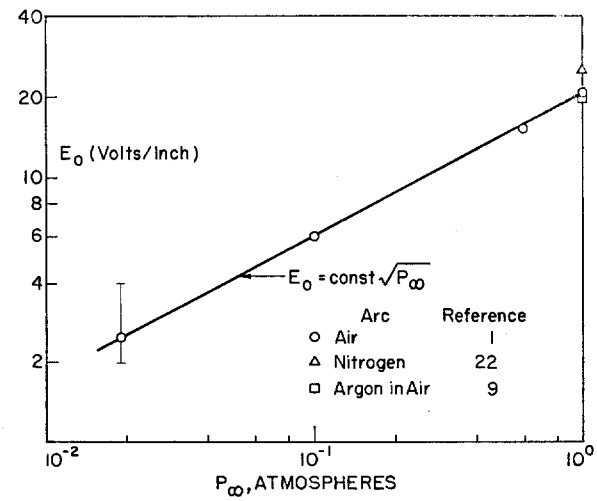

FIG. 12. Voltage gradient along a free-burning arc without cross flow.

[21] W. Finkelnburg and H. Maecker, in *Handbuch der Physik*, S. Flügge, Ed. (Springer-Verlag, Berlin, 1956), Vol. XXII, p. 254.

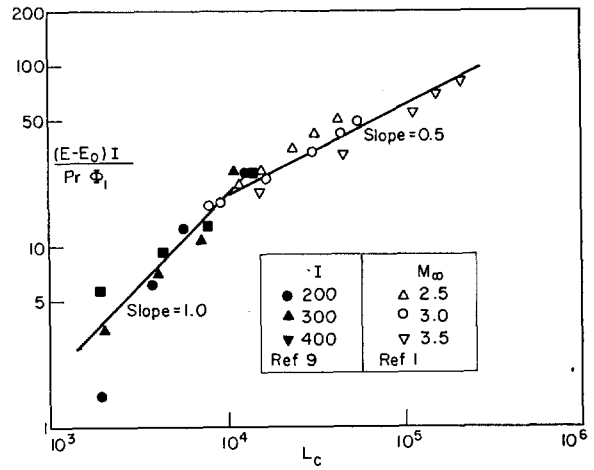

FIG. 13. Correlation of parameter for heat loss by forced convection.

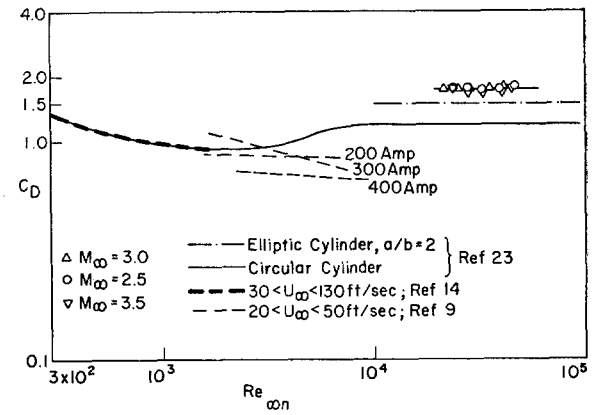

FIG. 14. Correlation of measured drag coefficient for solid cylinders with normal forced coefficients for arcs.

data extends the results of other investigations[9,22] to low pressures. In the absence of a cross flow, the heat generated, $E_0 I$, is transferred to the arc boundary by conduction and then to the surrounding medium, largely by free convection. If we assume that, for the range of arc currents used, the fields of the free-burning and blown arcs may be superimposed, we may write

$$E = E_0(P_\infty) + E_c(P_\infty, U_{\infty n}, I),$$

where the relative magnitudes of E_0 and E_c are determined by the relative importance of conduction and convection in transferring heat to the arc boundary, that is, at low L_c, $E \to E_0$ and, for high L_c, $E \to E_c$.

Figure 13 shows that the supersonic and subsonic data of Fig. 11 tend to collapse into a single curve when E_c is substituted for E. For $L_c < 10^4$ the data (except at the lowest L_c) cluster around a linear relationship between $E_c I/\Phi_1$ Pr and L_c while for $L_c > 10^4$ the relation is near the 0.5 power.

Accordingly, the plots of Figs. 11–13 support the hypothesis that Eqs. (15) and (16) describe, to a first approximation, the physical processes within the core of a balanced arc at Lorentz numbers greater than about 10^4. Further, since for the supersonic measurements $E_0 \ll E$ (see Fig. 6) and for the subsonic $E_0 \simeq 0.7$ to $0.9E$, the free-burning characteristics appear to dominate the transfer from the arc in the Roman–Myers experiments.

Some further insight into the validity of the gross features of the model of Sec. III and of the measured dimensions is given by considering the two-dimensional drag coefficient

$$C_d = BI/q_{\infty n}\, d_T, \tag{19}$$

where $q_{\infty n} = \frac{1}{2}\rho_\infty U_{\infty n}^2$, as plotted in Fig. 14 for the present measurements along with those of other investigations.[9,14] The agreement among the three sets of data as compared with the measured values for unheated circular cylinders[23] is quite remarkable considering divergences in the experimental conditions.[24]

The drag coefficient was nearly constant at 1.75 for the three supersonic Mach numbers, slightly higher than that for an elliptical cylinder at incompressible speeds.

The drag coefficient in Fig. 14 is plotted versus $\mathrm{Re}_{\infty n} = \rho_\infty U_{\infty n}\, d_1/\mu_\infty$, but the experimental results indicate that $\mathrm{Re}_{\infty n} \sim \mathrm{Re}$ for constant P_∞ and T_∞, that is, from Eqs. (12) and (19)

$$\frac{V_1}{U_{\infty n}} = \left(\frac{C_d}{2}\frac{\rho_\infty}{\rho_1}\frac{d_T}{d_1}\right)^{1/2}. \tag{20}$$

This ratio is nearly constant for the three supersonic Mach numbers and for the subsonic tests (Fig. 10). Since d_T/d_1 is nearly constant (Fig. 5), Eq. (20) indicates that ρ_1/ρ_∞ is nearly constant for the separate sets of data. Then

$$\mathrm{Re}_{\infty n} = \mathrm{Re}\,\frac{U_{\infty n}}{V_1}\frac{\rho_\infty}{\rho_1}\frac{\mu_1}{\mu_\infty}.$$

Since μ_1 depends on T_1, which varies only slightly for

[22] L. A. King, in *Proceedings of the 5th International Conference on Ionization Phenomena in Gases*, H. Maeche, Ed. (North-Holland Publishing Company, Amsterdam, 1962), Vol. I, p. 100.

[23] S. F. Hoerner, *Fluid Dynamic Drag* (published by S. F. Hoerner, Midland Park, New Jersey, 1965).

[24] Some of the divergences are: in all cases the arc deviated strongly from circular cross section; the experiments of Ref. 9 were carried out in a free jet with ratios of arc to jet width up to about 0.5; those of Ref. 14 were carried out in a closed channel; those reported here were carried out at near-sonic $U_{\infty n}$ on a strongly slanted arc.

a given P_∞ and T_∞ (Fig. 7), we have a relation between the internal and external similarity parameters for constant P_∞ and T_∞, that is,

$$\mathrm{Re}_{\infty n} \sim \mathrm{Re} = (L_c)^{1/2}. \tag{21}$$

Some further relations follow.

Since T_1 is nearly constant for a given T_∞ and P_∞ (Fig. 7),

$$d_1 \sim (I/E)^{1/2} \tag{22}$$

and Eq. (18) for large L_c becomes

$$K_{JH} = \text{const} = \frac{EI}{\Phi_1 \,\mathrm{Pr}\,(L_c)^{1/2}} \sim \frac{E^{3/2}\, I^{1/2}}{U_{\infty n}}$$

so that

$$E \sim U_{\infty n}^{2/3}/I^{1/3} \tag{23}$$

then Eq. (22) becomes

$$d_1 \sim I^{2/3}/U_{\infty n}^{1/3} \tag{24}$$

and, using Eq. (19) with C_d constant and $d_T \sim d_1$, we get, at large L_c for constant P_∞ and T_∞

$$B \sim U_{\infty n}^{5/3}/I^{1/3}. \tag{25}$$

As has been pointed out the above results apply to the *steady* balanced arc. An important problem still to be solved relates to the conditions governing the steadiness. As was mentioned in Sec. IID some runs showed slight unsteadiness, but in the main the arc was either quite steady, as shown by the photographs and the measured properties, or violently unsteady.

V. BOUNDARY-LAYER PROPERTIES

In Sec. III it was pointed out that at high values of the Lorentz parameter L_c the approximate momentum and energy equations [Eqs. (15) and (16)] are of the boundary-layer type. While, on the basis of the usual boundary-layer consideration (Pr near unity), one would also conclude that enthalpy and velocity boundary layers are of nearly equal thickness, it is shown below that the effect of the coupling between Joule heating and the Lorentz force will be to thin the inner portion of the enthalpy layer.

This coupling, expressed by Eqs. (15) and (16), may be described as follows. As a plasma element moves under the action of the pressure and Lorentz forces its temperature increases at the rate given by the excess of the Joule heating rate over the rate of transfer out of the element by conduction. Since the energy supply is limited, the temperature of the element will increase until the element arrives in the region where $\nabla^2\phi$ is large enough to cool it to the zero conductivity level. At the point where the enthalpy is a maximum $\mathbf{u}\cdot\nabla h = 0$ and Eq. (16) becomes

$$\left[\nabla^2\phi\right]_{h_{\max}} = -\frac{EI}{\Phi_1}\, j. \tag{26}$$

This point of maximum enthalpy may reasonably be taken as the inner edge of the boundary layer so that, since $j = J/J_1$ is near unity throughout the core, the value of $-EI/\Phi_1$ is approximately $\nabla^2\phi$ at the core boundary. Considering the range of values in Fig. 11, if, for instance, we take $EI/\Phi_1 = 50$ and a representative length interval $\Delta s = 0.1 d_1$, the experiments indicate that $\Delta\phi/\Delta s$ changes from zero to -0.5 over the distance Δs. Thus, the coupling between the heating of an element and the force acting on it leads to high-energy gradients at the upstream boundary.

The result can be made roughly quantitative as far as the dependence on Lorentz parameter is concerned. We first observe that, since Prandtl number and ϕ vary only slightly (Fig. 7), the plot of Fig. 11 indicates that EI, the rate of heat transfer from the arc, varies with $(L_c)^{1/2}$. Then, by use of Eq. (21), EI will be proportional to $\mathrm{Re}_{\infty n}$, and, since most of the transfer will occur at the upstream boundary, the relative thickness of the inner portion of the enthalpy boundary layer δ_h' will vary roughly as

$$\delta_h' \sim 1/\mathrm{Re}_{\infty n} \sim 1/(L_c)^{1/2}. \tag{27}$$

The thickness of the outer or electrically nonconducting portion of the boundary layer will be determined by the external flow and by the circumstance that the forced convection must carry away heat at the rate specified by Eq. (26). Therefore, the entire enthalpy layer thickness will approximately satisfy the relation of Eq. (27).

Cowley[14] analyzed a balanced arc, neglecting the effect of Joule heating and assuming that the thicknesses of the velocity and enthalpy boundary layers vary inversely with $(\mathrm{Re}_{\infty n})^{1/2}$. His over-all deductions are in fair agreement with subsonic experiments[14] at low Reynolds (Lorentz) numbers.

VI. CONCLUSIONS

Results given here on tests at supersonic speeds support the previous conclusion that the steady balanced arc at sub- and supersonic speeds comprises an impervious core and a boundary layer through which mass, energy, and momentum are transferred to the external flow. Some specific aspects of the fluid mechanical structure are:

(1) At supersonic cross flows the results are consistent with a model of the arc core in which the plasma is treated as a weakly ionized gas with negligible radiation and nonequilibrium effects.

(2) For the analysis of the internal circulation the results confirm the conclusion in Ref. 3 that a characteristic velocity proportional to the normal component of the external flow exists; the proportionality factor depends weakly on Mach number for supersonic speeds and is constant over a range of subsonic speeds.

(3) For circulation within the core, the most important nondimensional parameter is the "Lorentz parameter," analogous to the Grashof number in natural convection problems. The Lorentz parameter is approximately proportional to the square of the Reynolds number for the external flow past the arc.

(4) The supersonic results presented here satisfy the limiting condition at high Lorentz parameter for the simplified model, in that the relation between the Lorentz and Joule heating parameters is that required by the energy equation.

(5) The subsonic results of Ref. 9 do not satisfy this limiting condition, but a smooth interpolation with the supersonic results obtains when the effect of the transfer from the arc with no cross flow is taken into account; that is, when the voltage drop along the free-burning arc is subtracted from that measured in a cross flow at the same ambient pressure.

(6) The coupling between the heating and the Lorentz force on an element causes the inner portion of the enthalpy layer over the upstream arc boundary to vary inversely with the external Reynolds number, instead of with its square root, as would occur in the absence of the coupling

ACKNOWLEDGMENTS

The authors acknowledge the assistance and collaboration of Robert L. Harvey, particularly in connection with the photographs of Fig. 2 and for Fig. 9, and the help of Ronald Kapnick and C. W. Kauffman in taking and analyzing data. The advice and collaboration of Professor Richard L. Phillips on various aspects of arc physics and on the computor solutions, and of Professor Stuart W. Bowen on the taking and interpretation of optical data, are gratefully acknowledged.

The research was supported in large part by National Aeronautics and Space Administration Grant NGR-23-005-128.